JVI
Journals.ASM.org

The Myristate Moiety and Amino Terminus of Vaccinia Virus L1 Constitute a Bipartite Functional Region Needed for Entry

Chwan Hong Foo,[a] J. Charles Whitbeck,[b] Manuel Ponce-de-León,[a] Wan Ting Saw,[a] Gary H. Cohen,[a] and Roselyn J. Eisenberg[b]

Department of Microbiology, School of Dental Medicine,[a] and Department of Pathobiology, School of Veterinary Medicine,[b] University of Pennsylvania, Philadelphia, Pennsylvania, USA

Vaccinia virus (VACV) L1 is a myristoylated envelope protein which is required for cell entry and the fusion of infected cells. L1 associates with members of the entry-fusion complex (EFC), but its specific role in entry has not been delineated. We recently demonstrated (Foo CH, et al., Virology 385:368–382, 2009) that soluble L1 binds to cells and blocks entry, suggesting that L1 serves as the receptor-binding protein for entry. Our goal is to identify the structural domains of L1 which are essential for its functions in VACV entry. We hypothesized that the myristate and the conserved residues at the N terminus of L1 are critical for entry. To test our hypothesis, we generated mutants in the N terminus of L1 and used a complementation assay to evaluate their ability to rescue infectivity. We also assessed the myristoylation efficiency of the mutants and their ability to interact with the EFC. We found that the N terminus of L1 constitutes a region that is critical for the infectivity of VACV and for myristoylation. At the same time, the nonmyristoylated mutants were incorporated into mature virions, suggesting that the myristate is not required for the association of L1 with the viral membrane. Although some of the mutants exhibited altered structural conformations, two mutants with impaired infectivity were similar in conformation to wild-type L1. Importantly, these two mutants, with changes at A4 and A5, undergo myristoylation. Overall, our results imply dual differential roles for myristate and the amino acids at the N terminus of L1. We propose a myristoyl switch model to describe how L1 functions.

Poxviruses are unique DNA viruses that replicate in the cytoplasm and employ a multifaceted form of morphogenesis (18). Vaccinia virus (VACV) is the prototype virus that has been used to study the replication of poxviruses (40, 48), and in an attenuated form the virus was deployed as a vaccine for the global eradication of smallpox (30, 39). Multiple infectious forms of VACV are produced during viral replication. The majority of the infectious progeny virions are single-enveloped mature virions (MV), which form adjacent to virus replication sites and are released only by cell lysis.

During the initial step of entry, the MV utilizes four envelope proteins, A27, H3, D8, and A26, to mediate attachment to a variety of cell surface molecules, such as heparan sulfate proteoglycan (HSPG) (16, 44), chondroitin sulfate proteoglycan (34), and the extracellular matrix protein laminin (15). After adsorption, the virion can use pH-dependent or pH-independent pathways to enter cells (6, 14, 47, 60, 83). The specific viral proteins responsible for receptor binding, virus internalization, the triggering of virus-cell fusion, and membrane fusion itself are poorly defined. Components of a conserved, multiprotein entry-fusion complex (EFC) are proposed to perform certain nonredundant functions that are critical for entry (8, 11, 38, 52, 53, 61, 64–66, 76–78, 85). Eleven proteins have thus far been identified to form the massive complex (A28, H2, A21, L5, G3, G9, A16, J5, O3, F9, and L1), and each polypeptide component, with the exception of O3 and J5, has been demonstrated to be essential for the penetration of the viral core into the cytoplasm and for VACV-induced cell-cell fusion, a surrogate process for VACV-cell fusion (8, 11, 38, 52, 53, 61, 64–66, 76–78, 85). I2 is another envelope protein that is required for penetration (51), and it is considered a candidate as the 12th member of the EFC.

The absence of some of the components of the EFC results in the disassociation of the other components (65), implying that intricate intermolecular interactions mediate either the assembly or structural integrity of the EFC. The known exceptions are L1 and F9. The absence of either protein does not prevent the formation of the rest of the EFC (8, 11). Thus far, neutralizing antibodies have been raised against three subunits of the EFC: L1 (2, 32, 35, 86), A28 (24, 49), and F9 (11). L1-specific antibodies have the most potent activity. MAbs to L1 diminish VACV-induced cell-cell fusion (37), strongly neutralize infectivity (2, 36, 37, 71, 86), and inhibit virus entry (24, 83). In sum, these attributes suggest that L1 is not merely a structural scaffold for the EFC. Rather, it is more likely that L1 plays a more active and dynamic role during entry.

L1 is a 250-amino-acid (aa) myristoylated polypeptide with a predicted C-terminal transmembrane domain that spans residues 186 to 204 (25, 26). The N-terminal region is considered to be the ectodomain which is exposed on the surface of the MV (55). Two structures of the nonacylated form of the L1 ectodomain have been solved by X-ray crystallography (70, 71). The truncated protein has five α-helices packed against two double-stranded β-sheets, as well as a disorganized C-terminal tail which is proximal to the predicted membrane-anchoring domain (Fig. 1A). We showed that L1 fulfills two of the criteria for a viral receptor-binding protein (RBP): (i) soluble forms of L1 block virus entry at the adsorption step, and (ii) the protein binds to cell surfaces (24). These attributes are in contrast to those of the EFC constituent A28, which was not able to fulfill either criterion. Although L1 binds to cells lacking glycosaminoglycans like A27, it is different

Received 1 November 2011 **Accepted** 29 February 2012
Published ahead of print 7 March 2012
Address correspondence to Chwan Hong Foo, chfoo@upenn.edu.

doi:10.1128/JVI.06703-11

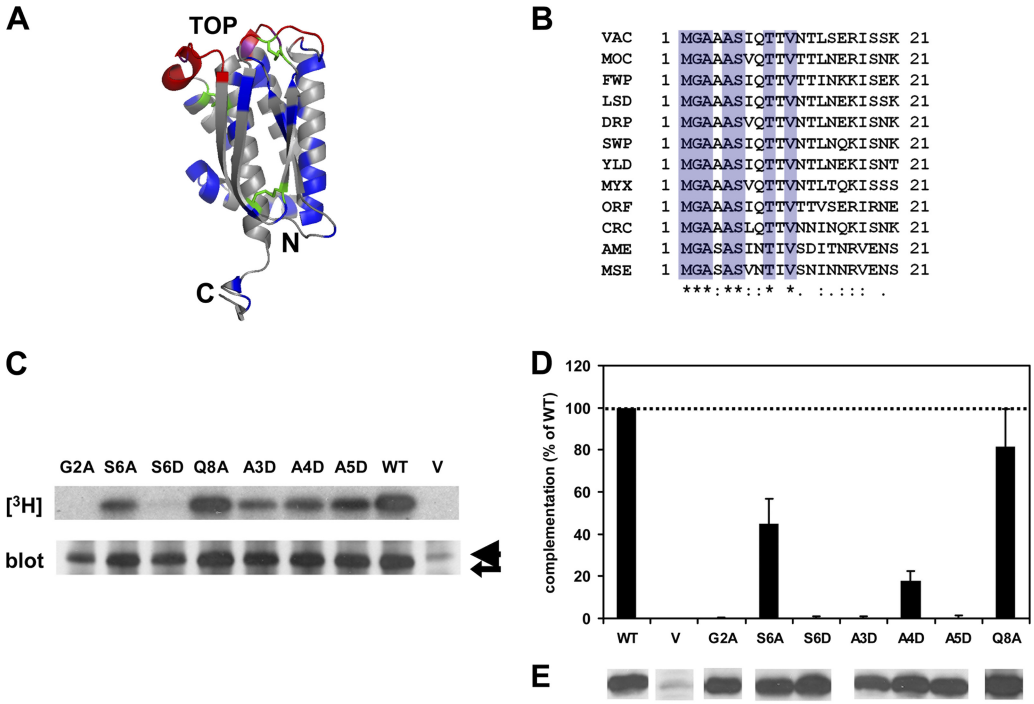

FIG 1 Mutations in conserved N terminus of L1 are deleterious for complementation of infectivity and N-myristoylation. (A) Crystal structure of the ectodomain of L1 (70). A ribbon representation of the right-side view of the structure is depicted. Residues which are conserved among poxvirus orthologs of L1 (blue) and the cysteines involved in disulfide bonding (green) are highlighted. The neutralizing epitopes (red) of L1 (2), including that of the MAb 7D11 (71), were mapped primarily to three discontinuous loops which are distal from the C-terminal transmembrane region. (B) Multiple-sequence alignment of residues 1 through 21 of VACV L1 with orthologs of other poxviruses. Orthologs of L1 that are representative of each chordopoxvirus genus, two entomopoxviruses, as well as deerpox virus and crocodilepox virus are shown (http://www.poxvirus.org/). VAC, VACV; MOC, molluscum contagiosum virus; FWP, fowlpox virus; LSD, lumpy skin disease virus; DRP, deerpox virus; SWP, swinepox virus; YLD, Yaba-like disease virus; MYX, myxoma virus; ORF, orf virus; CRC, crocodilepox virus; AME, *Amsacta moorei* entomopoxvirus; MSE, *Melanoplus sanguinipes* entomopoxvirus. The stars, dots, and colons below the alignment indicate the degree of conservation. Seven out of 21 of the N-terminal residues (blue) in L1 are strictly conserved in the sequences of all aligned poxvirus orthologs. (C) Mutations in the canonical myristoylation motif of L1 suppress myristoylation, while mutations in other conserved residues do not abrogate myristoylation. Cells were infected with the conditional L1-null virus vL1Ri in the absence of IPTG. Cells were then transfected with an empty vector (V) or plasmids encoding wild-type (WT) or mutant forms of L1. Cells were radiolabeled with [9,10-^{3}H]myristic acid and lysed, and immunoprecipitations were performed using a polyclonal IgG raised against recombinant L1 (R180). Immunoprecipitated radiolabeled proteins were then resolved by SDS-PAGE and visualized by fluorography (top panel). The expression of L1 (arrow) was also assessed by chemiluminescence after Western blotting with R180 (bottom panel). Note that the light chain of IgG (arrowhead) migrates proximally above L1. (D) Mutations in the N terminus of L1 prevent the complementation of infectivity. Cells were infected with vL1Ri in the absence of IPTG. Cells were then transfected with an empty vector (V) or plasmids encoding wild-type (WT) or mutant forms of L1. Crude cell extracts were harvested, and infectious virus titers were determined by standard plaque assays in the presence of IPTG. All data depicted are average values from at least five independent experiments. Error bars represent standard deviations of the means. (E) Protein expression of L1 in the extracts used for titration was determined by chemiluminescence after Western blotting with R180.

from A27 in its ability to block entry in these glycosaminoglycan-deficient cells. We postulated that L1 functions in VACV entry by engaging host receptor(s) which are not proteoglycans.

In this report, our goal was to identify novel structural regions of L1 which are essential for its functions in entry. We constructed L1 mutants and tested their ability to complement infectivity, to be myristoylated, and to associate with the EFC. The results show that the conserved amino terminus of L1 constitutes a bipartite region essential for proper protein function. Certain residues in this region are important for the N-myristoylation of L1, while other amino acids are critical for infectivity but not for myristoylation. We also found that the myristate moiety is not required for the incorporation of L1 into mature virions or for its association with the EFC. We propose a novel myristoyl switch model to explain how L1 functions.

MATERIALS AND METHODS

Cells and viruses. BSC-1 cells were grown in Dulbecco's modified Eagle's medium (DMEM) containing 10% fetal calf serum (FCS).

VACV vL1Ri (Western Reserve strain no. AY243312) (8), a recombinant virus with an inducible L1R gene regulated by the T7 promoter and *lac* operator, was used for assays requiring transient complementation. For the preparation of purified virus, BSC-1 cells were infected at a multiplicity of infection (MOI) of 0.05 PFU/cell in 50 μM isopropyl β-D-1-thiogalactopyranoside (IPTG) until cytopathic effect was complete (3 to 4 days). Virions were then harvested from the cells and purified by sucrose gradient sedimentation, as described previously (2). Titers were determined by plaque assay with BSC-1 cells. vL1Ri was a gift from B. Moss (8). VACV vSIJC-20 (Western Reserve strain no. NC_006998) was a gift from S. N. Isaacs.

Production and purification of proteins for antibody production. (i) Recombinant baculovirus proteins VACV H2, A21, and L5. The H2R, A21L and L5R open reading frames (ORFs) were PCR amplified from the respective cloned HindIII H, A, and L fragments of the VACV (Western Reserve strain no. NC_006998) genome (S. N. Isaacs, unpublished data). The putative transmembrane domains of the full-length H2R (residues 32 to 48), A21L (residues 1 to 19), and L5R (residues 30 to 47) ORFs were excluded, and their ectodomains (residues 49 to 189, 23 to 117, and 48 to 128, respectively) were expressed. For H2, the forward primer used for

PCR amplification was 5′-GCG**GGATCC**ACACCACCACCACCACCAC CAGACGTCTGATAATCCAGTCTTT-3′ (adds six histidine codons [underlined] to the 5′ end of H2R ORF as well as a BamHI site [boldface]), and the reverse primer was 5′-GCG**GGTACC**TATTCCATATTACTAAA AT-3′ (adds KpnI [boldface]). For A21, the forward primer used for PCR amplification was 5′-GCG**GGATCC**ACACCACCACCACCACCACTCT GAAAAAATGAGACGCGAAC-3′ (adds six histidine codons [underlined] to the 5′ end of the A21L ORF as well as a BamHI site [boldface]), and the reverse primer was 5′-GCG**GAATTC**AGGTAGTAAAAAATAAG TC-3′ (adds EcoRI [boldface]). For L5, the forward primer used for PCR amplification was 5′-GCG**GGATCC**ACACCACCACCACCACCACAGA TCTGAATTAAATATGTTC-3′ (adds six histidine codons [underlined] to the 5′ end of the L5R ORF as well as a BamHI site [boldface]), and the reverse primer was 5′-GCG**GAATTC**ATCTGCGAAGAACATCGTTAA G-3′ (adds EcoRI [boldface]).

The final PCR products were digested with either BamHI and EcoRI or BamHI and KpnI and subsequently ligated into the baculovirus transfer plasmid pVT-Bac (74), which was digested with the same set of restriction enzymes. Therefore, the resulting recombinant plasmids contained ORFs consisting of the melittin signal sequence followed, in frame, by the six histidine codons and the ectodomain of H2 (codons 49 to 189), A21 (codons 23 to 117), or L5 (codons 48 to 128).

The resulting pVT-Bac plasmids encoding recombinant H2, A21, and L5 were cotransfected with baculovirus DNA (BaculoGold; BD-Pharmingen) into Sf9 insect cells. After 1 week, recombinant baculoviruses were harvested. The viruses then were plaque purified and high-titer stocks were prepared (59). The recombinant proteins were secreted from infected insect cells and purified from supernatants using nickel-chelate affinity chromatography, as described previously (59). The identities and purities of the purified proteins were confirmed by Western blotting and silver stain (Pharmacia) analysis, respectively.

(ii) L1(2-34) peptide. Peptides were synthesized by Peptide 2.0, Inc. (Chantilly, VA). The peptides were purified by high-pressure liquid chromatography (HPLC; 220 nm; SinoChrom ODS-BP), resulting in purities higher than 95%. They were dissolved in 50% dimethyl sulfoxide (DMSO) in deionized H_2O prior to use. The sequence used for the wild-type (WT) peptide consists of residues 2 to 34 of L1 (GAAASIQTTVNTL SERISSKLEQEANASAQTKC), while the sequence of the scrambled form of the same peptide was SLLEQEANSGASEATSKIAQTKCASRIQTTVN.

PAbs and monoclonal antibodies (MAbs). Rabbit polyclonal antibodies (PAbs) R202, R206, R208, and R251 were produced by immunizing rabbits with purified recombinant H2, A21, and L5 proteins and L1(2-34) peptide, respectively, using procedures described previously for raising PAbs (24). Preimmune antibody (control) was harvested from a rabbit prior to immunization. The production of rabbit PAb R180, raised against recombinant L1(185t), was reported previously (2, 20). The production of PAbs R193 and R204, raised against recombinant A27 and A28, respectively, also was reported in a previous study (24), while R236 was raised against peptides derived from the VACV A4 core protein (83).

MAbs VMC-2, VMC-3, and VMC-35 were selected from a panel of monoclonal antibodies against purified recombinant L1 (2). MAb 7D11, raised against VACV, was kindly provided by A. L. Schmaljohn (A. L. Schmaljohn, J. W. Hooper, and S. A. Harrison, unpublished data) (86). The anti-tetrahistidine MAb was purchased from Qiagen, Inc., while antibodies to caveolin-1 (mouse MAb clone 2297) and early endosomal antigen 1 (mouse MAb clone 14) were obtained from BD Transduction Laboratories. The anti-c-myc MAb 9E10 (21) was used as a negative control for immunoprecipitations.

Immunoglobulin G (IgG) was purified from rabbit sera and murine ascites fluid with HiTrap protein G 1-ml columns (Amersham Pharmacia Biotech) and dialyzed against phosphate-buffered saline (PBS). The PAb R180 was biotinylated using the EZ-Link Sulfo-NHS-Biotin kit (Thermo Scientific). Horseradish peroxidase (HRP)-conjugated anti-mouse and anti-rabbit secondary antibodies were from Kirkegaard and Perry Laboratories.

Construction of L1 expression plasmids. For the construction of the pEndoL1 (WT) plasmid, the L1R open reading frame with its endogenous promoter region beginning from the −40 position (TTATCTCTCTTGG TAATATGGATACTAATTGTAGCTATTTAA) was amplified by PCR using DNA from VACV vSIJC-20 (Western Reserve strain no. NC_006998) (S. N. Isaacs, unpublished data) as the template. The forward primer used for PCR amplification was 5′-GCTTATCTCTCTTGGTAAT ATGG-3′, and the reverse primer was 5′-TCAGTTTTGCATATCCGTG GTAG-3′. The PCR product was then cloned, using TOPO TA cloning, into the pCR2.1-TOPO vector (Invitrogen, CA). The QuikChange II site-directed mutagenesis kit (Stratagene Cloning Systems) was used to generate plasmids from template pEndoL1 (WT) that contained single-residue point mutations. The L1R open reading frame and the promoter region in each plasmid were sequenced to screen out PCR errors.

Transient complementation of L1-null virus. BSC-1 cells were grown to confluence in 6-well plates and infected with gradient-purified vL1Ri at an MOI of 5. The infection media lacked antibiotics. At 1 h postinfection (hpi), the cell monolayers were transfected with either vector DNA (circularized pCR2.1; Invitrogen) or plasmid DNA encoding either wild-type L1R (pEndoL1) or a mutant form of L1R. DNA (0.5 μg) was mixed with 6 μl of Lipofectamine 2000 (Invitrogen) in a total volume of 0.5 ml of Opti-MEM I reduced-serum media (Invitrogen) per well. At 6 hpi, the transfection mix was replaced with fresh medium containing antibiotics.

At 24 hpi, the infected and transfected cells were harvested and centrifuged at 1,200 × *g* for 10 min at 4°C, and supernatant was aspirated. The cell pellets were lysed in cold, hypotonic 10 mM Tris-HCl (pH 9.0) buffer. Efficient cell lysis was ensured by freeze-thawing the samples three times with alternating −80 and 37°C cycles. Lastly, the samples were sonicated for 1 min, and cell debris was removed by centrifugation at 1,200 × *g* for 10 min at 4°C. The crude virus supernatant, consisting of the complemented virus, was stored at −80°C for subsequent steps.

To determine the ability of the transfected L1R construct to rescue the infectivity of vL1Ri, a plaque assay was performed in the presence of a chemical inducer of the *lac* operon. The virus supernatant was serially diluted in medium with 50 μM isopropyl β-D-1-thiogalactopyranoside (IPTG). One hundred μl of diluent was added to each well in duplicate in a 48-well plate cultured with confluent BSC-1 cells. The monolayers were incubated with the diluent at 37°C for 1 h, and then 400 μl of fresh media and IPTG were added. At 18 hpi, the infected cells were fixed with 2.5% formaldehyde in PBS, plaques were visualized by staining with 0.1% crystal violet, and then they were counted. After the subtraction of background values (titer of virus complemented with vector DNA), the complementation efficiency of each mutant construct was represented as a percentage of the titer of virus complemented with wild-type L1R DNA (pEndoL1). Results are typically an average of a series of at least five independent experiments.

SDS-PAGE and Western blotting. Crude virus supernatants of mutant virions were first prepared as described in the previous section. Total proteins were then separated by SDS-PAGE under reducing (boiled for 5 min in 60 mM Tris-HCl, 1% SDS, 10% glycerol, 20 mM dithiothreitol [DTT]) conditions in 12% precast Tris-glycine gels (Invitrogen). DTT was absent from experiments performed under nonreducing conditions. Following SDS-PAGE, separated proteins were transferred to nitrocellulose membranes. Membranes were then incubated with blocking solution overnight at 4°C and probed with 0.5 μg/ml of the IgG PAb or the appropriate MAb. After three rinses with PBS containing 0.2% Tween 20, blots were reacted for 1 h with secondary antibody (goat-anti-mouse or goat-anti-rabbit) coupled to HRP, diluted in PBS containing 5% nonfat dry milk and 0.2% Tween 20. Following more rinses with PBS containing 0.2% Tween 20, chemiluminescence was activated by the addition of ECL substrate (Pierce Biotechnology, IL) and visualized using X-ray film (Thermo Scientific Fisher). For experiments performed under nonreducing conditions, the protein bands were analyzed by densitometry using ImageJ software (1).

Metabolic radiolabeling with [^{3}H]myristic acid. The standard transient complementation protocol was performed, and at 12 hpi the cells were refed with fresh DMEM supplemented with low-FCS content (2.5%). Radiolabeled [9,10-^{3}H]myristic acid (1.0 mCi/ml; 50.5 Ci/mmol; Perkin Elmer, MA) was prepared by drying under argon gas and resuspending in DMSO with brief sonication. Aliquots of 225 μl of the working solution were added to the cells in each well. Cells were labeled from 12 to 24 hpi with an estimated 28 μCi activity per well. At 24 hpi, cells were harvested in extraction buffer, and immunoprecipitation was done as described below, except that 10 μg/ml of R180 IgG was used instead.

Each immunoprecipitated sample was divided into two equivalent portions, one for fluorography and the other for Western blotting. Protein samples of both portions were resolved by SDS-PAGE under reducing conditions in 12% Tris-glycine gels. Separated proteins were either fixed overnight in 40% ethanol–10% acetic acid (vol/vol) solution in preparation for fluorography or transferred to nitrocellulose and reacted with biotinylated R180 primary and HRP-conjugated strepavidin secondary antibodies. Chemiluminescence was then recorded using X-ray film. For fluorographic analysis, the fixed gels were immersed in Amplify fluorographic reagent (Amersham Biosciences) for 30 min and then dried by vacuum. Radiolabeled proteins were visualized by exposing the gels to Kodak Biomax MS film with a BioMax TransScreen LE intensifying screen at −80°C for periods of up to 60 days. A subset of fluorographs was analyzed by densitometry using ImageJ software (1).

Protein incorporation in mature virions. BSC-1 cells were grown to confluence in T-225 flasks and infected with gradient-purified vL1Ri at an MOI of 5. The infection medium consisted of DMEM containing 10% FCS without antibiotics. At 1 hpi, the cell monolayers were either mock transfected or transfected with vector DNA or plasmid DNA encoding either wild-type L1R (pEndoL1) or a mutant form of L1R. Eleven μg of DNA was mixed with 88 μl of Lipofectamine 2000 in a total volume of 11 ml of Opti-MEM I reduced-serum medium per flask. At 6 hpi, the transfection mix was replaced with antibiotic-supplemented fresh medium.

At 24 hpi, the infected and transfected cells were harvested and lysed by freeze-thaw in hypotonic 10 mM Tris-HCl (pH 9.0) buffer, and intracellular mature virions were purified by sucrose gradient sedimentation, as described previously (2). The samples of purified vL1Ri were analyzed by Western blotting using antibodies to L1 (R180), A4 core (R236), caveolin-1, or early endosomal antigen 1.

Immunoprecipitation with monoclonal antibodies. Transient complementation of L1-null virus was performed as described above. At 24 hpi, the cells were harvested by centrifugation and lysed on ice by the addition of extraction buffer (10 mM Tris, pH 8.0, 150 mM NaCl, 10 mM EDTA, 1% NP-40, 0.5% sodium deoxycholate, 1× Complete protease inhibitor cocktail [Roche Applied Science, IN]). The samples were sonicated, and cell debris as well as nuclei were removed by centrifugation at 10,000 × *g* for 15 min at 4°C. Ten μg/ml of VMC-3, VMC-2, VMC-35, 7D11, or anti-myc MAb IgG was added, and the lysate-antibody mix was incubated overnight at 4°C. Agarose beads conjugated to protein A (Invitrogen) then were incubated with the lysate-antibody mix for 2 h at 4°C. Following two rinses with extraction buffer and one rinse with TE buffer (10 mM Tris-HCl, pH 8.0, 1 mM EDTA), the bound proteins were solubilized by the addition of SDS sample buffer (final concentration of 60 mM Tris-HCl, 1% SDS, 10% glycerol, 20 mM DTT) and by boiling for 5 min.

Immunoprecipitated proteins and whole-cell lysates (WCL) were resolved by SDS-PAGE under reducing conditions in 12% Tris-glycine gels, transferred to nitrocellulose, and then probed with a biotinylated antibody to L1 (biot-R180). Membrane-bound biotinylated IgG was reacted against streptavidin-HRP conjugate (GE Healthcare) at a 1:5,000 dilution in PBS containing 3% bovine serum albumin (BSA) (Fraction V; Roche) and 0.2% Tween 20. Chemiluminescence was imaged using X-ray film.

Coimmunoprecipitation of L1 with members of the entry-fusion complex (EFC). Following the transient complementation of L1-null virus, the cells expressing mutant forms of L1 were harvested in EFC coimmunoprecipitation lysis (ECIL) buffer (50 mM Tris, pH 8.0, 150 mM NaCl, 1% NP-40, 0.1% SDS, and 1× Complete protease inhibitor cocktail) at 24 hpi. Immunoprecipitation was done using 10 μg/ml of R180 IgG in ECIL buffer. Immunoprecipitated proteins and whole-cell lysates were separated by SDS-PAGE under reducing conditions in 12% (for blots probed for L1) or 14% (for blots probed for A27, A28, H2, A21, and L5) Tris-glycine gels. Resolved proteins were blotted onto nitrocellulose and then detected with rabbit PAb to A27 (R193), A28 (R204), H2 (R202), A21 (R206), L5 (R208), or L1 (biot-R180). Membrane-bound antibodies were reacted against HRP-conjugated anti-rabbit antibodies or streptavidin-HRP conjugates. Chemiluminescence was imaged by exposure to X-ray films.

ELISA. Purified VACV vSIJC-20 (8×10^6 PFU per well) or 50 μl of 3% BSA in PBS was added to 96-well plates. For the enzyme-linked immunosorbent assays (ELISAs) using peptides, 1 μg per well of L1(2-34) peptides with either the wild-type or scrambled primary sequence was added. After 1 h at room temperature (RT), the plates were washed with PBS, blocked with PBS containing 5% nonfat dry milk and 0.1% Tween 20, and then probed with 5 μg/ml of R180 or R251 diluted in the blocking solution for 1 h at RT. Following more rinses with PBS, plates were further incubated for 30 min with goat anti-rabbit secondary antibody coupled to HRP diluted 1:1,000 in blocking solution. After the final washing step with PBS containing 0.1% Tween 20, the wells were rinsed once with 20 mM citrate buffer, pH 4.5. 2,2′-Azinobis(3-ethylbenzthiazolinesulfonic acid) (ABTS) peroxidase substrate was added, and the absorbance at 405 nm was measured with a plate reader.

Inhibition of virus entry by antibodies. Purified immunoglobulins from anti-L1 PAb R180, anti-L1(2-34) PAb R251, or preimmune sera were serially diluted in DMEM containing 5% heat-inactivated FCS and then mixed with an equal volume of reporter virus VACV vSIJC-20. The virus-antibody mixture was incubated for 1 h at 37°C and then used to infect BSC-1 cells at an MOI of 2.5 PFU/cell in 96-well plates. After 6 h at 37°C, β-galactosidase expression was assessed as a measure of entry as described previously (24).

RESULTS

Mutations in the canonical myristoylation motif of L1 prevent efficient myristoylation and complementation of a conditional L1-null virus. One conserved region within L1 and its homologous proteins is its amino terminus (Fig. 1A). Excluding the initiating methionine, 6 of the 10 amino-terminal residues are strictly conserved among poxvirus orthologs from all genera, including those of the distantly related insect poxviruses and the unclassified reptilian crocodilepox virus (Fig. 1B) (http://www.poxvirus.org/). This suggests that this segment performs a functional role, prompting us to focus our current study on this portion of L1.

Two residues, G2 and S6, match the consensus motif for N-terminal myristoylation (G-X-X-X-S/T) (Fig. 1B) (10, 22). Previous reports have demonstrated that viral L1 undergoes N-terminal myristoylation at glycine 2 (25, 26), and that myristoylation was inhibited when glycine 2 was replaced with alanine (26, 54). Additionally, the first 13 N-terminal residues of L1 are required for myristoylation within the context of a chimeric protein (54). L1 is required for the entry and fusion of VACV (8, 24), but the role of its myristate group is unclear.

To investigate the role of the myristate moiety, we first constructed mutant forms of L1 by manipulating its canonical myristoylation motif. Using PCR-based genetic mutagenesis, we generated the previously reported nonmyristoylated mutant G2A (26, 54). Another study investigating the amino acid requirements for the N-myristoylation of a prototypical protein demonstrated that the lipid modification, while tolerant of an alanine substitution at position 6, is abrogated by replacement with valine, aspartic acid,

lysine, or arginine at this position (79). Hence, we constructed two mutants at S6, changing it to either aspartic acid (S6D) or alanine (S6A).

We also developed a transient complementation assay which utilizes a conditional L1-null virus, vL1Ri (8), to enable the expression of L1 within its natural physiological context. In the absence of the chemical inducer IPTG, the expression of the endogenous genomic L1R gene by the mutant virus was inhibited by the *lac* repressor. A plasmid encoding a mutant form of L1 was subsequently introduced into vL1Ri-infected cells in *trans* by transient transfection. The expression of the mutant L1 was regulated by its natural late promoter and thus is activated in infected cells.

Once the assay was optimized, we evaluated whether the mutant proteins would undergo myristoylation during infection. vL1Ri-infected cells were transfected with plasmids expressing wild-type L1, G2A, S6A, or S6D and metabolically radiolabeled with [9,10-^{3}H]myristic acid. Radiolabeled L1 from cell lysates was immunoprecipitated with an L1-specific polyclonal antibody (PAb) (Fig. 1C). The Western blotting of the immunoprecipitated L1 verified that similar amounts of mutant and wild-type L1 were loaded (Fig. 1C, lower). An intense radiographic band corresponding to the migration of L1 in an SDS gel was present in the lane loaded with wild-type L1 (Fig. 1C, upper). In contrast, the band was absent from the lanes which were loaded with G2A or the empty vector (Fig. 1C, upper). The replacement of serine 6 with alanine (S6A) permitted myristoylation, whereas replacement with a charged residue (S6D) essentially abolished myristoylation. These results are consistent with the study which delineated the myristoylation requirements of a prototypical protein (79). Our results demonstrate that the canonical myristoylation motif (G-X-X-X-S/T) exists within the conserved amino terminus of L1.

We next assessed the ability of each mutant protein to restore virus infectivity in *trans*. Progeny mutant virions from the complementation assay were harvested, and the number of plaques was determined for virions complemented with wild-type L1, mutant forms of L1, or the empty vector. IPTG was added at this step to allow plaque formation. Western blotting confirmed that the mutated proteins were expressed at levels similar to those of wild-type L1 (Fig. 1E). The two nonmyristoylated mutants, G2A and S6D, failed to complement virus infectivity (Fig. 1D). The myristoylated mutant S6A restored about half of the infectivity restored by wild-type L1 ($P < 0.05$ by Student's *t* test). For these three mutants, the capacity of each mutant to complement infectivity correlates with the extent of myristoylation. We conclude that the myristoyl group of L1 is essential for its proper protein function.

Mutations in other conserved N-terminal residues of L1 are deleterious for complementation but not for myristoylation. Several residues in the N terminus do not belong to the canonical myristoylation motif (Fig. 1B), but they may affect myristoylation or play an alternative role for L1 function. Two (A3 and A5) are conserved among poxvirus orthologs from different genera, and two (A4 and Q8) are conserved in noninsect poxviruses (Fig. 1B). To investigate their functions, glutamine 8 was exchanged with alanine (Q8A) to eliminate the polar side chain, while alanines at positions 3, 4, and 5 were replaced with aspartic acid (A3D, A4D, and A5D).

Figure 1C shows that these mutations had minimal effects on L1 myristoylation. Interestingly, most of these mutations had drastic effects on infectivity (Fig. 1D). The replacement of alanine at positions 3 to 5 either abolished or significantly compromised the ability of L1 to complement infectivity ($P < 0.05$ by Student's *t* test). Again, the defects in complementation are not due to inadequate protein expression (Fig. 1E). Q8A, on the other hand, rescued infectivity to levels which are not significantly different from that of wild-type L1 ($P > 0.05$ by Student's *t* test).

Collectively, our results demonstrate the presence of two independent, important structural motifs within the N terminus of L1: (i) the attached myristate moiety and (ii) the residues from positions 3 to 5.

The myristate moiety is not required for the incorporation of L1 into mature virions. The myristate moieties of some cytosolic proteins of other viruses are necessary for the efficient incorporation of the proteins into maturing or budding virions (27, 42, 63, 82). The lipid group acts as an anchor for protein-membrane association by its insertion into the inner leaflet of the viral envelopes. It has been proposed that the L1 myristate is needed for the targeting of the protein to the correct viral membrane during morphogenesis (7, 56).

We used purified, complemented mutant virions to determine whether the myristate group is necessary for the incorporation of L1 into virions. Cell extracts from a scaled-up version of the transient complementation system were collected and clarified. Virions were then purified by ultracentrifugation through sucrose gradients. The relative level of the viral core antigen A4 was used to normalize the quantity of virus for each construct (Fig. 2A, top). Using L1-specific R180 antibodies, we found that the nonmyristoylated proteins, G2A and S6D, were present in virions (Fig. 2A). We also assayed for cellular proteins to verify virion purity (Fig. 2A, bottom). We did not detect either the host membrane protein caveolin-1 or EEA1, an early endosomal antigen. Thus, even though the myristoylation of L1 is essential for complementation, it is not necessary for the localization of L1 to virions.

We next considered whether the mutants which are myristoylated but exhibited defects in infectivity were incorporated into mature virions. It is possible that the mutant proteins, due to aberrant folding, were mislocalized from specialized membranes in the viral factories to other subcellular compartments (7). We detected the mutant proteins S6A and A3D (Fig. 2A), as well as A4D and A5D (Fig. 2B), in the purified virions. Thus, the inability of these mutants to function in the complementation assay is not attributable to a trafficking or packaging deficiency.

Mutations in the canonical myristoylation motif result in changes in structural conformations. Bisht et al. used confocal immunofluorescence microscopy to demonstrate that the conformationally dependent MAb 7D11 fails to bind to intracellular G2A (7). We wondered whether the other epitopes of G2A were affected and whether our other nonmyristoylated mutant, S6D, would exhibit similar epitope changes. We therefore carried out a more comprehensive analysis of the structure-conformation of our mutants. Three conformation-dependent MAbs, two of which neutralize virus, were included in our analysis. We employed the immunoprecipitation approach rather than confocal microscopy, as it allows for a more quantitative analysis. These MAbs target different epitopes, since they do not compete with one another for binding to the protein (2). In the structure, the epitopes of the two neutralizing MAbs (VMC-2 and 7D11) map to a region distant from the amino terminus (2, 71), while the epitope of VMC-35 is unknown. The conformation-independent MAb VMC-3 was incorporated in the analysis as a positive control

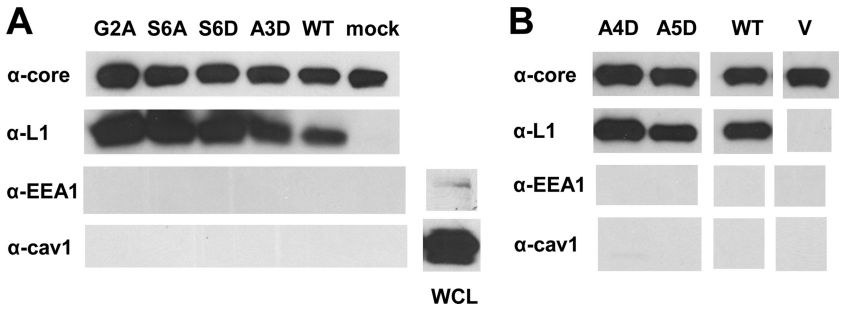

FIG 2 N-terminal mutants of L1 are incorporated into mature virions. (A) The myristate group is not required for the efficient incorporation of L1 into virions. Cells were infected with vL1Ri in a T-225 flask and then mock transfected (A) or transfected with an empty vector (V) (B), plasmids encoding wild-type (WT) L1, or mutant forms of L1. Cell lysates were collected and processed into clarified supernatants. Mature virions were purified by the ultracentrifugation of the supernatants in stepwise sucrose gradients. The amount of the viral core protein A4, L1, caveolin-1, or EEA-1 incorporated in the virions was determined by Western blotting with a polyclonal IgG raised against an A4 peptide (R236), R180, or MAbs specific for the cellular antigens. Caveolin-1 or EEA-1 present in unprocessed lysates (WCL) of infected cells was also blotted (lower right panels). (B) Virion packaging of A4D and A5D was also assessed in another independent experiment using the method described for panel A.

(2). It binds to a linear peptide derived from residues 118 to 128 of L1.

Both of the nonmyristoylated mutants, G2A and S6D, were reactive with 7D11 but at reduced levels, and they lost their ability to bind VMC-35 (Fig. 3A). Hence, epitopes from two different regions, one of which is distant from the N terminus (71), were modified in these mutants. We also analyzed the third mutant which had an amino acid substitution in its myristoylation motif. The myristoylated S6A was recognized by both 7D11 and VMC-35, although its reactivity to the latter MAb was decreased. The difference in antibody reactivity profile between S6D and S6A may explain why S6A was able to restore infectivity to a greater extent than S6D in the complementation assay (Fig. 1D). All three mutants were detected by VMC-2 but not by the negative control MAb to Myc.

Bisht et al. also reported that G2A is in a reduced redox state (7). Based on the atomic structure of L1 in complex with 7D11 (71), the loss of the Cys34-Cys57 disulfide bond, specifically, is

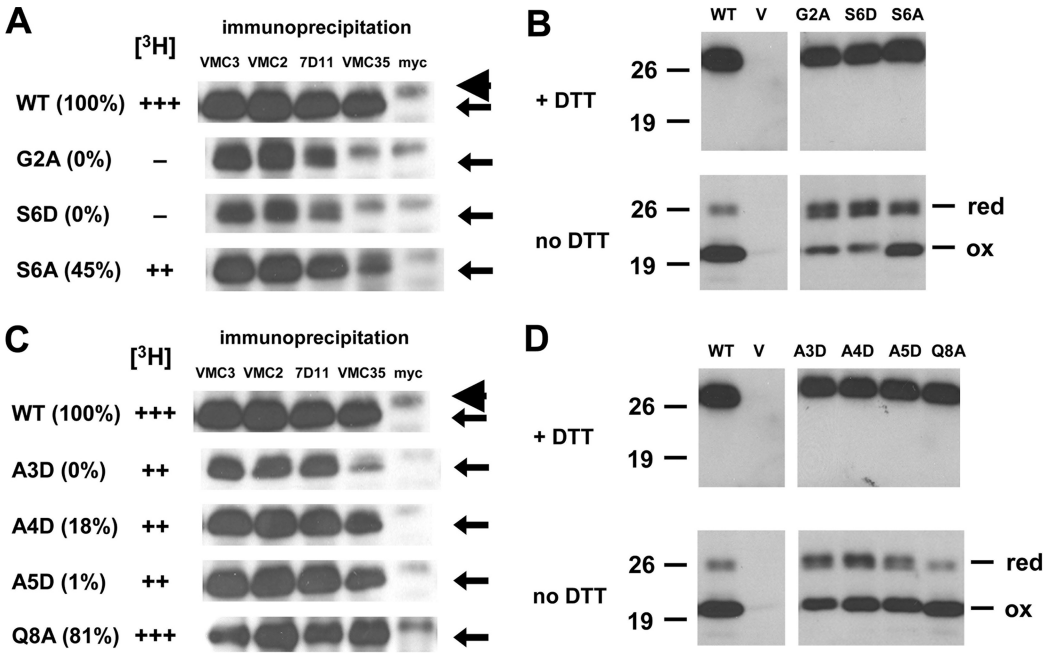

FIG 3 Mutations in the myristoylation motif (A and B) and other conserved N-terminal residues (C and D) result in changes in structural conformations. vL1Ri-infected cells were transfected with plasmids encoding wild-type (WT) or mutant forms of L1. (A and C) Cell lysates were harvested and immunoprecipitations were performed using conformation-specific MAb to L1 (VMC-2, 7D11, or VMC-35), a conformation-independent MAb to L1 (VMC-3), or a nonspecific control MAb (anti-myc). The amount of L1 (arrows) bound to the MAbs was then determined by Western blotting with a biotinylated polyclonal IgG raised against L1 (biot-R180), along with a streptavidin-HRP conjugate. Note that the light chain of IgG (arrowhead) migrates proximally above L1. The complementation efficiency of each mutant is depicted in parentheses as a percentage of the wild-type level. The relative myristoylation efficiency ([^{3}H]) of each mutant is also illustrated. (B and D) Analysis of the redox state of the mutants. Lysates of cells were electrophoresed under denaturing conditions (boiled for 5 min in 60 mM Tris-HCl and 1% SDS), either in the presence (top) or absence (bottom) of DTT. The proteins were transferred to nitrocellulose and then probed using R180. The reduced (red) and oxidized (ox) forms of L1 are labeled accordingly.

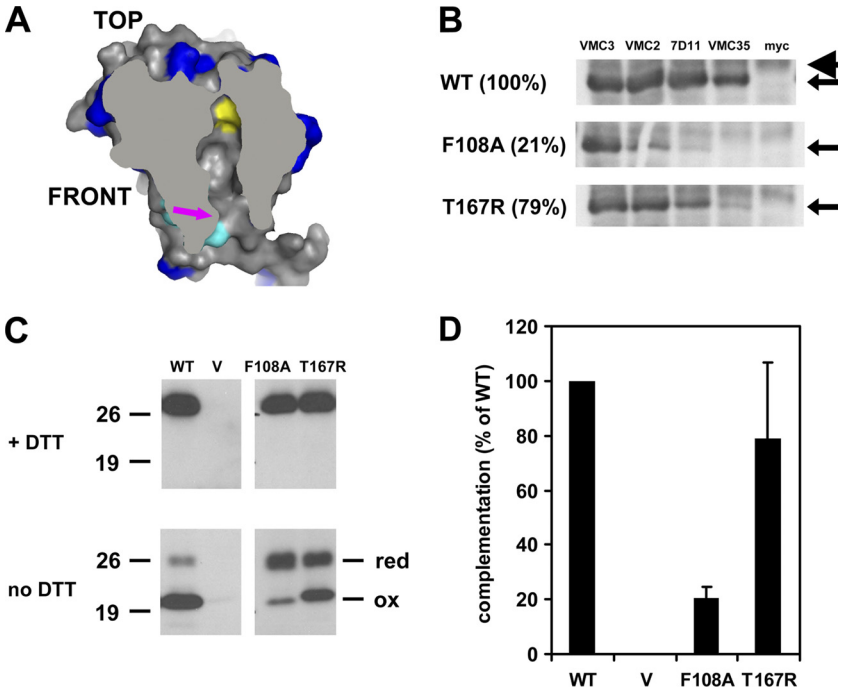

FIG 4 Characterization of the conserved hydrophobic residue within the cavity of L1 (F108). (A) Hydrophobic pocket within the structure of L1. Surface representation of the cross-sectional view of the structure. The conserved residue F108 (yellow) is situated close to the end of the cavity. Residues which are conserved among poxvirus orthologs of L1 (blue) and the first four N-terminal residues (cyan) are depicted, along with the opening to the cavity (arrow). (B) Conformational epitopes of F108A are dissimilar from those of wild-type L1. Lysates of infected cells transfected with plasmids encoding wild-type L1 (WT) or F108A were generated. Immunoprecipitations were performed using conformation-specific MAb to L1 (VMC-2, 7D11, or VMC-35) or anti-myc. The amount of L1 (arrows) bound to the MAbs was then determined by Western blotting with biot-R180. The light chain of IgG (arrowhead) migrates above L1. (C) The majority of F108A is not fully disulfide bonded. Lysates of complemented cells were electrophoresed under denaturing conditions, either in the presence (top) or absence (bottom) of DTT. The proteins were transferred to membranes and then probed with R180. (D) F108A, but not T167R, is impaired in its ability to restore the complementation of infectivity. Infected cells complemented with L1 were lysed, and infectious virus titers were determined by plaque assays. Error bars represent standard deviations of the means.

likely to destabilize the 7D11 epitope (data not shown). It has been shown that all three of the disulfide bonds of L1 are important for its function (9). We therefore investigated the redox state of our mutants, as it is likely that the tempered recognition of S6D by 7D11 is also due to the absence of disulfide bonding in the mutant. The three mutants were analyzed by SDS-PAGE either in the presence or absence of DTT, followed by Western blotting with an L1-specific PAb. In agreement with the discovery by Bisht et al. (7), we found that the majority of G2A is not fully disulfide bonded (Fig. 3B, bottom). Under nonreducing conditions, doublet bands of G2A migrated at a distance similar to that of the 26-kDa marker protein. This distance is similar to that migrated by G2A under reducing conditions (Fig. 3B, top), when it exists as only a single band. As such, the upper band of this doublet probably represents the completely reduced form of L1, while the lower band belongs to a partially reduced form, since three disulfide bonds exist in L1 (Fig. 1A).

Interestingly, the other nonmyristoylated mutant, S6D, presented migration and density profiles that are almost identical to those of G2A (Fig. 3B). Employing relative densitometry, we ascertained that the doublets of S6D and G2A accounted for an estimated 66 and 63%, respectively, of the total density of all bands belonging to each mutant protein. In contrast, only approximately 17% of the total density of wild-type L1 was present in its doublet bands. Correspondingly, the partially myristoylated mutant S6A exhibited patterns which appear to be an intermediate between those of the nonmyristoylated mutants and of wild-type L1.

These observations indicate that alterations in the canonical myristoylation motif, G2 and S6, can induce structural and biochemical changes in L1. Interestingly, these changes include the 7D11 epitope that is spatially distant from the N terminus (Fig. 1A) (71).

A conserved hydrophobic residue within the cavity of L1 is important for native conformation and complementation. An internal hydrophobic cavity is present within the ectodomain of L1 (Fig. 4A). Computational modeling has shown that this cavity can accommodate a myristic acid molecule (70). In addition, the cavity opening is close to the amino terminus, where the lipid is attached (54). Thus, the crystallographers who solved the structure of L1 proposed that the myristoyl group is buried within this pocket, at least in one of its conformational states (70). According to this model, more than one of the hydrophobic residues lining the internal surfaces of this pocket should be critical for shielding the fatty acid from the solvation shell during protein folding. Reducing the hydrophobicity of such a residue, or the removal of the entire myristate, would likely destabilize the hydrophobic packing of L1 and alter its discontinuous epitopes.

Among the residues lining the wall of the cavity, F108 is one of the most universally conserved and hydrophobic (Table 1). The unique properties of its aromatic ring may also strengthen intramolecular interactions within L1, perhaps via dispersion forces

TABLE 1 Residues which line the wall of the internal cavity of L1[c]

Residue	Position	Conservation[a] (%)	Hydropathy scale[b]
V	11	100	4.2
L	79	100	3.8
F	108	100	2.8
Y	76	92	−1.3
T	10	83	−0.7
V	104	67	4.2
L	163	67	3.8
I	7	58	4.5
L	14	58	3.8
A	72	58	1.8
T	75	58	−0.7
V	87	58	4.2
A	170	58	1.8
T	167	50	−0.7
F	91	25	2.8
L	166	25	3.8
M	90	8	1.9

[a] Based on the alignment of the sequence of VACV L1 with 11 representative sequences of orthologs from different poxvirus genera.
[b] Hydrophobicity values as described by Kyte and Doolittle (43).
[c] See reference 70.

TABLE 2 Densitometric analysis of fluorograph of [^{3}H]myristic acid-labeled F108A

Construct	Density		
	Absolute mean[a]	Relative mean[b]	Relative (as % of WT)
WT	0.772	0.06	100
V	0.712	0	0
F108A	0.757	0.045	75

[a] The absolute mean density is normalized to the background density of the fluorograph.
[b] The relative mean density is obtained by subtracting the absolute density of the vector from each absolute density.

between its electron cloud and the alkyl groups of the sequestered myristate (Fig. 4A; also see Fig. 7). To assess the significance of F108, we generated a mutant with an alanine substitution. Alanine is still a hydrophobic residue, but it lacks an aromatic ring (43). We carried out MAb immunoprecipitation, gel electrophoresis under nonreducing conditions, and complementation of the infectivity of F108A. We found that the structural conformation of F108A, as well as its function, differs significantly from those of wild-type L1 (Fig. 4). First, the binding of F108A to VMC-2 and 7D11 were significantly reduced, while its binding to VMC-35 was essentially undetectable by immunoprecipitation (Fig. 4B). The loss of MAb binding only applies to conformational antibodies, since the pulldown of F108A by the conformation-independent MAb VMC-3 was possible. Second, the majority of the mutant protein is not fully disulfide bonded (Fig. 4C). Relative densitometry indicates that the upper doublet of F108A, which likely represents two different reduced redox species, accounted for an estimated 75% of the total density of all bands of L1. In stark comparison, roughly less than 17% of the total density of wild-type L1 was present in its doublet. Unsurprisingly, F108A was drastically impaired in its capacity to restore infectivity ($P < 0.05$ by Student's t test) (Fig. 4D). On the other hand, the mutation of threonine 167, which also lines the cavity wall (Table 1), to a charged residue (T167R) did not significantly diminish complementation relative to that of the wild type ($P > 0.05$ by Student's t test) (Fig. 4D). Immunological and biochemical analyses of T167R correspondingly indicate that relative to F108A, the structural details of this mutant are more wild type like (Fig. 4B and C).

We conclude that F108 is uniquely important for the native conformation of the protein and for its proper function. These two characteristics of F108A are reminiscent of those of the nonmyristoylated mutants, G2A and S6D. However, F108A could be metabolically radiolabeled with tritiated myristic acid (Table 2). Hence, in contrast to G2A and S6D, the defect exhibited by F108A in complementation is not due to an absent acyl chain. Rather, the observed phenotypes of F108A are consistent with the proposed model that the myristate is normally sequestered within the hydrophobic hole of L1.

The myristate moiety is not required for the association of L1 with members of the entry-fusion complex. Myristoyl groups have been documented to mediate protein-protein interactions directly by acting as a binding motif (13, 46, 72). L1 is a peripheral component of the multiprotein VACV entry-fusion complex (EFC) (8), but the domains on L1 responsible for its association with the complex have not been identified. One possible alternative model for the structural location of the myristate posits that the lipid is instead embedded inside a hydrophobic pocket of an associated EFC protein, and thus it serves as an interaction motif for the EFC. We thus used our nonmyristoylated mutants to ascertain whether they fail to associate with the EFC proteins. If this alternative model is correct, it may explain why these mutants are impaired in complementation. In fact, mutants of the EFC constituent H2, which lose their association with EFC partners, are concomitantly defective in infectivity (50), suggesting that preserving the coassociation of EFC subunits is vital for VACV infectivity.

We used coimmunoprecipitation to appraise the association of the nonmyristoylated mutant G2A with the EFC. Infected-transfected cells were lysed, and immunoprecipitations were performed using an L1-specific PAb or a nonspecific control antibody to Myc. Blots were probed with PAbs to each respective viral antigen. This allowed us to detect the amount of L1, A27, or EFC proteins expressed in cells or captured in the antigen-antibody complex.

As expected, G2A and wild-type L1 were expressed in the whole-cell lysate (Fig. 5A, top). Similar amounts of G2A and wild-type L1 were found when they were first immunoprecipitated and then Western blotted with anti-L1 IgG R180 (Fig. 5A, middle). Thus, the G2A mutation did not affect the binding of R180 to L1. The non-EFC viral protein A27 was also detected in the whole-cell lysate (Fig. 5B, top), but as expected, it was not coimmunoprecipitated with L1 (Fig. 5B, middle). This confirmed the specificity of the coimmunoprecipitation. In contrast, the EFC subunits A28 (Fig. 5C, middle), H2 (Fig. 5D), A21 (Fig. 5E), and L5 (Fig. 5F) coimmunoprecipitated with G2A, and they did so at levels similar to that of the wild-type counterpart. The control MAb did not capture the EFC proteins (Fig. 5, bottom), indicating that the detection of each of the EFC components was dependent upon the presence of L1 in the pulldown mix. Comparable results were acquired with the partially myristoylated mutant S6A (Fig. 5). In a separate experiment, the nonmyristoylated mutant S6D also coimmunoprecipitated with the EFC proteins A28 and H2 (data not shown). Thus, the myristoyl moiety of

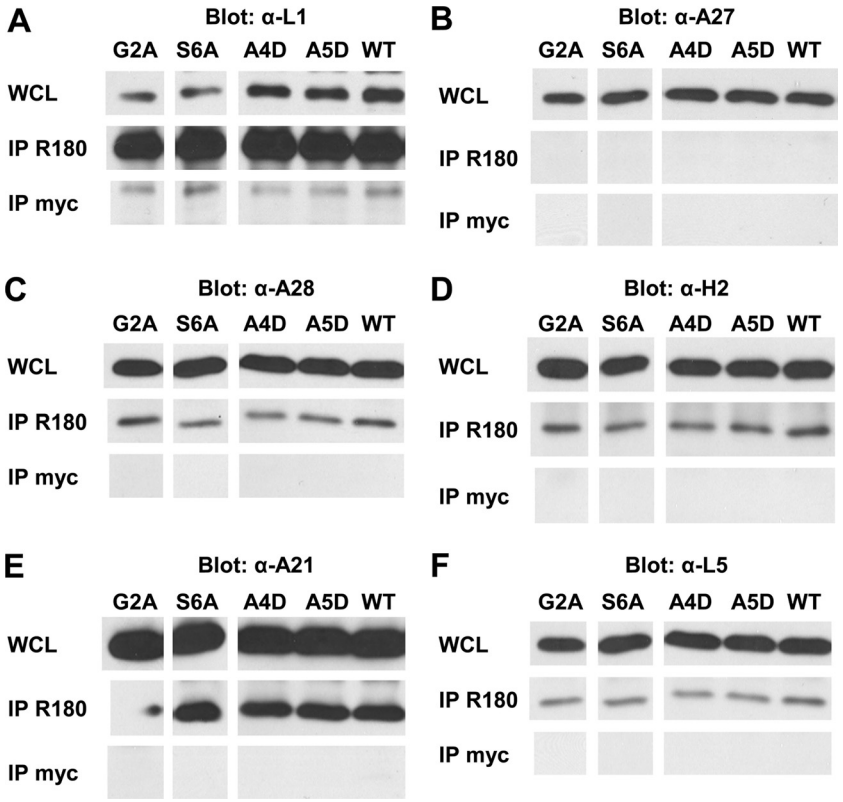

FIG 5 N-terminal mutants remain in association with the VACV EFC. vL1Ri-infected cells were transfected with plasmids encoding wild-type (WT) or mutant forms of L1. (Top panels) Whole lysates of these cells (WCL) were electrophoresed and blotted with antibodies specific for each viral protein: biot-R180 for L1 (A), R193 for A27 (B), R204 for A28 (C), R202 for H2 (D), R206 for A21 (E), and R208 for L5 (F). (Middle panels) Immunoprecipitations of the lysates were also performed using R180 (IP R180). The amount of L1, A27, or members of the EFC coimmunoprecipitated with the R180 IgG was determined by Western blotting with antibodies specific for each protein. (Bottom) Immunoprecipitations were performed using a nonspecific control MAb, anti-myc (IP myc). The amount of L1, A27, or members of the EFC bound to the control MAb IgG was ascertained by Western blotting.

L1 is not required for its association with any of the EFC proteins studied here. These observations are more consistent with the structural model for L1, where its lipid group is sequestered within the cavity (Fig. 4A; also see Fig. 7). In addition, it can be stated that the defective complementations observed for these mutants were not caused by their loss of interaction with the EFC.

The inability of A4D and A5D to function is not attributable to changes in their structural conformations or the loss of association with the entry-fusion complex. Earlier we showed that the other N-terminal mutants, A3D, A4D, and A5D, were myristoylated (Fig. 1C) and incorporated into purified virions (Fig. 2), but they were impaired in their ability to complement virus infectivity (Fig. 1D). To verify that these mutants retained their native conformations, we attempted to immunoprecipitate them with the conformation-dependent MAbs used to assess the nonmyristoylated mutants. Interestingly, the three mutant proteins exhibited different MAb reactivity profiles (Fig. 3C). First, the replacement of A3 with aspartic acid did not significantly affect binding with VMC-2 and 7D11, but its reactivity with VMC-35 was appreciably diminished. In contrast, the antibody binding profiles of A4D and A5D were similar to that of wild-type L1. Furthermore, when we assessed the redox state of A4D and A5D by nonreducing gel electrophoresis, the relative densities of bands of the reduced and oxidized species suggest that the majority of each mutant possess proper disulfide bonding (Fig. 3D and data not shown). In sum, our results indicate that, unique among the mutants that show some defect in complementation, A4D and A5D retained their native conformational epitopes and are similar structurally to their wild-type counterpart (Table 3).

We subsequently wondered whether these mutants were defective in complementation, because they could no longer associate with their EFC partners. It is possible the conserved N terminus is a binding site for the EFC, and each of these alanines serves as a critical contact residue for binding. We first subjected the mutants A4D and A5D to the EFC coimmunoprecipitation analysis (Fig. 5). As with the previous set of mutants, both A4D and A5D coimmunoprecipitated with A28 (Fig. 5C, middle), H2 (Fig. 5D), A21 (Fig. 5E), and L5 (Fig. 5F). Similar results were also acquired for the mutant A3D in a separate experiment (data not shown). These observations indicate that the impairment of these mutants in complementation is not due to the loss of association with these subunits of the VACV EFC. The conserved amino-terminal residues A4 and A5 are therefore not necessary for the N-myristoylation of L1, proper structural conformation, or for EFC association of L1, but they play a critical role during virus entry.

Antibodies raised against a peptide derived from the N terminus of L1 do not neutralize virus entry. In a previous report, we proposed that L1 is a viable candidate for the canonical receptor-binding protein of VACV (24). Here, using substitution mutants, we have identified a novel functional region within the

TABLE 3 Properties of L1 mutants with N-terminal amino acid substitutions[d]

Substitution mutant	Complementation (% of WT)	MAb detection of discontinuous epitope:			N-myristoylation	Association with EFC[a]	Virion incorporation	Phylogenetic conservation of residue[b]
		VMC-2	7D11	VMC-35				
G2A	0	+ + +	+	−	−	+	+	All
A3D	0	+ + +	+ + +	+ +	+ +	+	+	All
A4D	18	+ + +	+ + +	+ + +	+ +	+	+	Chordopoxvirus only
A5D	1	+ + +	+ + +	+ + +	+ +	+	+	All
S6A	45	+ + +	+ + +	+ +	+ +	+	+	All
S6D	0	+ + +	+	−	−	+	+	All
Q8A	81	+ + +	+ + +	+ + +	+ + +	NT[c]	NT	Chordopoxvirus only
WT	100	+ + +	+ + +	+ + +	+ + +	+	+	

[a] As determined by the ability of the mutant to coimmunoprecipitate with A28, H2, A21, or L5.
[b] Most of the mutated residues are conserved in orthologs of L1 from all poxvirus genera, including the unclassified crocodilepox virus. A4 and Q8, however, are conserved only among chordopoxvirus orthologs.
[c] NT, not tested.
[d] The numbers of plus and minus signs represent quantitative differences in the data set.

extreme N terminus of L1 (Table 3). We therefore inquired whether the N terminus of L1 is the region responsible for the binding of L1 to cell surfaces and for its ability to inhibit VACV entry. We surmised that antibodies which target the N terminus of L1 should inhibit entry if this is the pertinent region.

Since none of the available L1-specific MAbs bind to the N terminus of L1 (2), we first designed a synthetic peptide comprised of residues 2 to 34 of L1 for polyclonal antibody production (Fig. 6A). To allow for the sulfhydryl coupling of keyhole limpet hemocyanin to the peptide during antibody generation, the Cys34 residue was the terminal residue included. The L1(2-34) peptide was also designed with the intention of preserving its native secondary structure. Both the resolved secondary structure of residues 2 to 34 of the L1 structure (70) and the computationally predicted secondary structure of the peptide (17) suggest that the peptide is primarily an α-helix flanked by coils at its termini (Fig. 6A). To first confirm that at least some of the epitopes present in VACV L1 are preserved in the L1(2-34) peptide, we performed an ELISA using R180, a PAb which was raised against soluble ectodomain L1. In this assay, peptides were coated on a microtiter plate and then serial dilutions of antibodies were added. The PAb R180 bound, in a dose-dependent fashion, to L1(2-34) peptides (data not shown). The binding was sequence specific, since the affinity of R180 for a peptide with the same amino acid composition but with a randomized order was significantly lower.

A polyclonal antibody (R251) was subsequently produced by immunizing a rabbit with purified L1(2-34) peptide, using procedures described previously for raising PAbs (24). Proteins from infected cell lysates were separated under reducing and denaturing conditions using SDS-PAGE, transferred to a nitrocellulose membrane, and then probed using immunoglobulin purified from rabbit sera R251 or R180 (Fig. 6B). R251 detected three major bands, with the fastest migrating band (~26 kDa) representing full-length viral L1. Additionally, the same antibody bound to the L1(2-34) peptide immunogen that was used to generate it, as well as to baculovirus-derived truncated L1 (data not shown). To verify that R251 recognizes full-length VACV L1 in its native context on the surface of virions, we performed a virus ELISA. A fixed amount of gradient-purified mature virions was added to a microtiter plate, and then increasing amounts of R251 or R180 IgG were used to probe the viral proteins. Figure 6C shows that R251 recognized plate-bound virions at a significantly lower apparent affinity than R180. The binding of both antibodies is dependent upon the presence of viral proteins, since they did not bind to bovine serum albumin (Fig. 6C, circles). The lower affinity exhibited by R251 relative to that of R180 is perhaps unsurprising, since the former was generated against a 33-amino-acid synthetic peptide while the latter was made against a glycosylated polypeptide with 185 residues (2).

Finally, the effect of R251 on the entry of VACV was tested using a β-galactosidase entry assay. This assay utilizes a recombinant VACV with the *lacZ* reporter gene regulated by a VACV early/late promoter (83). If the N terminus of L1 is the region responsible for the capacity of L1 to bind to cells and to suppress entry, the antibody should be able to neutralize the entry as well. We found that the immunoglobulin in fact did not affect virus entry (Fig. 6D). R180, on the other hand, virtually abrogated entry at 100 μg/ml. This suggests that the N terminus of L1, though constituting a critical functional region, is not the domain responsible for the ability of soluble L1 to impede VACV entry.

DISCUSSION

VACV L1 has demonstrated significant potential as an effective immunogen for vaccine candidates which are in development against lethal orthopoxvirus diseases (23, 31, 33, 87). Its significance is due to its ability to generate potent virus-neutralizing antibodies (2, 86). Our overall goal of this study was to further advance our fundamental understanding of this protein. In this study, we identified a novel structural region in the amino terminus of L1 which is essential for proper protein function. Interestingly, residues within this region are crucial for two different purposes. Some residues are important for the myristoylation of L1, while others play another critical role during entry that is distinct from myristoylation.

The role of the myristate moiety of L1. L1 was first discovered by Franke et al., who characterized the nature and extent of fatty acid modifications of VACV proteins (25). The radiolabeling of VACV-infected cells with tritiated myristic acid resulted in the identification of two major acylated viral proteins, one of which had an apparent molecular mass of 25 kDa. The authors later identified the myristoylated protein as the gene product of the VACV L1R ORF (26) and were the first to demonstrate that the

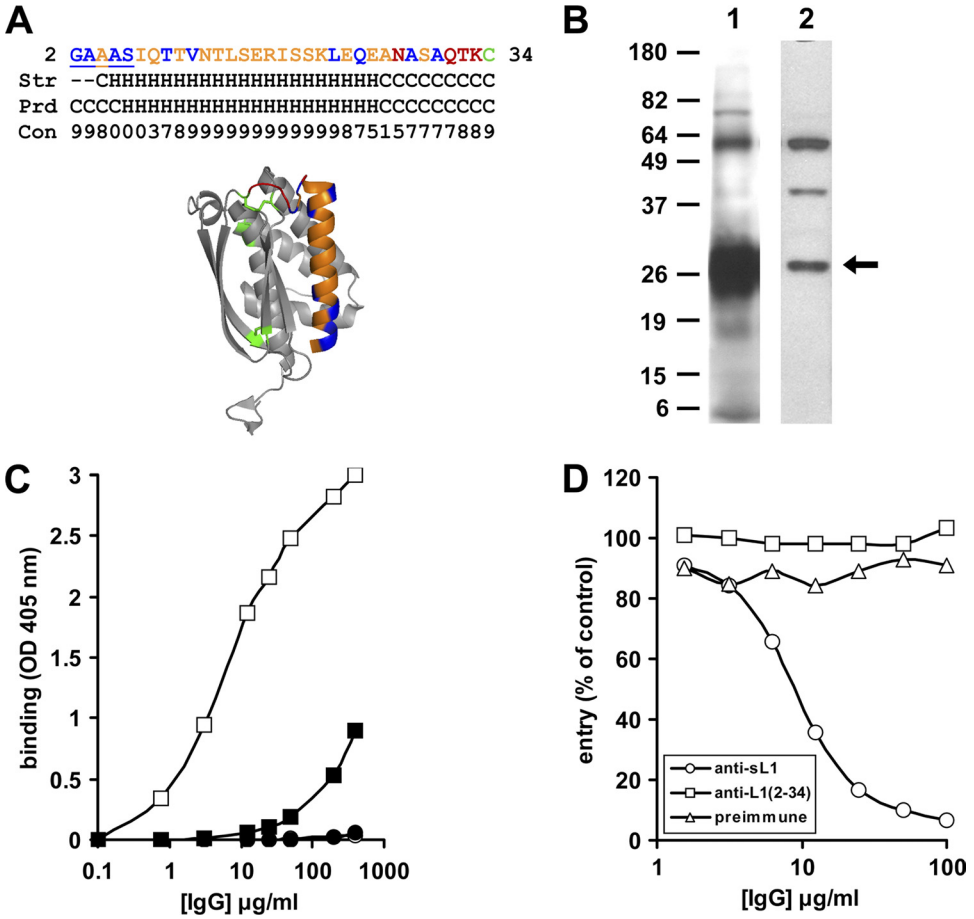

FIG 6 Antibodies raised against a peptide derived from N terminus of L1 do not neutralize virus entry. (A) A 33-amino-acid peptide derived from the N terminus of L1. The primary sequence of the peptide is shown (top), with residues which are important for complementation underlined. The peptide (orange) is also highlighted within the context of the ectodomain structure of L1 (bottom). The residues in the structure are color coded as described for Fig. 1A. The secondary structure of residues 2 to 34 in the ectodomain structure (Str) and the predicted secondary structure of the peptide (Prd) are listed, along with the confidence of prediction by the Jpred 3 bioinformatics tool (Con) (17). G2 and A3 of the crystal structure were not resolved (dash) (70). (B) The PAb raised against the L1(2-34) peptide detects VACV L1 from infected cells. Infected cells complemented with wild-type L1 were lysed. Lysate proteins were resolved by SDS-PAGE under denaturing conditions, transferred to membranes, and probed with R180 (lane 1) or R251 (lane 2). (C) R251 recognizes nondenatured purified virions. Purified vSIJC-20 virions (8×10^6 PFU per well) (squares) or 3% BSA (circles) was added to 96-well plates. An ELISA was then performed using serial dilutions of R180 (open symbols) or R251 (filled symbols) as the detection antibody. (D) R251 does not neutralize the entry of VACV. Multiple concentrations of anti-soluble L1 PAb (R180), anti-L1(2-34) PAb (R251), or preimmune IgG were preincubated with VACV vSIJC-20 for 1 h. The virus-antibody mix was then added to BSC-1 cells. At 6 hpi, the cells were lysed and β-galactosidase activity was measured.

alteration of its G2 residue to alanine or aspartic acid prevents the myristoylation of L1. In a separate study using chimeric mutants, the authors showed that the first 13 amino-terminal residues of L1 influence the efficiency of fatty acid conjugation (54).

In this study, we constructed novel mutations in the canonical myristoylation motif of L1. Congruently with the findings of Franke et al. (26), we first confirmed that a conservative replacement of the G2 residue with an alanine abrogated myristoylation. This is unsurprising, given that the α-amino group of the glycine is strictly required for the covalent conjugation of the myristate via an amide bond (22). In addition, we showed that although a relatively conservative change of the S6 residue to an alanine allowed for myristoylation, a less conservative change in S6 to aspartic acid completely abolished myristoylation. The availability of mutants with different myristoylation efficiencies subsequently allowed for the further delineation of the purpose of the myristoyl moiety.

First, the extent of the myristoylation of G2A, S6D, and S6A correlates with their capacity to complement virus infectivity (Table 3). The nonmyristoylated mutants G2A and S6D were unable to rescue infectivity in the complementation assay, while the partially myristoylated mutant S6A restored about half of the infectivity of wild-type virions. Employing a similar complementation assay, Ravanello and Hruby reported that the infectivity of the G2A mutant generated by their group was almost entirely ablated (approximately 2% of the wild type) (56). This phenotype was virtually identical to that of the mutant made by us (0% of the wild-type level of infectivity). These two studies showcase the importance of the myristate moiety for infectivity.

Second, we observed that the myristoylation efficiencies of G2A, S6D, and S6A correlate with the authenticity of their conformational epitopes and redox states. The majority of the nonmyristoylated mutants exist as redox species lacking at least one pair of the disulfide bonds that are critical for function (9). The redox profile of S6A, on the other hand, suggests that about half of

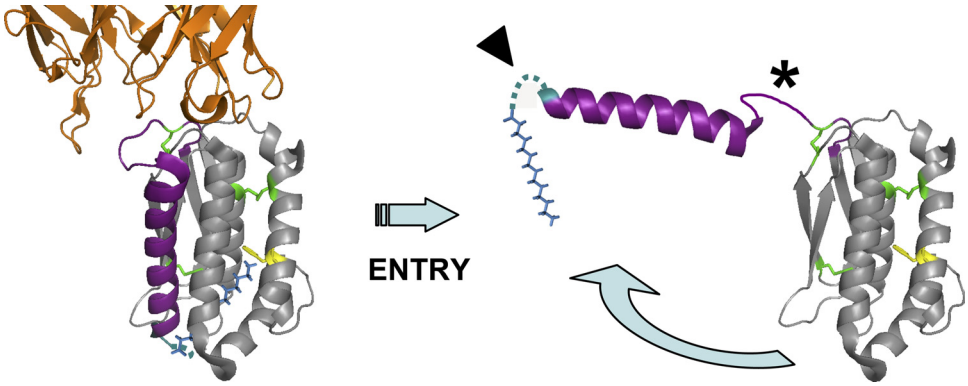

FIG 7 Myristoyl switch model for L1. Ribbon representation view of the left side of the L1 structure (71). In the rested conformational state (left), the myristate moiety (blue model) is buried internally within L1, possibly stabilized by the conserved residue F108 (yellow). Upon activation during entry, loop 1 (asterisk) acts as a hinge to swing α1 helix (purple) and its amino-appended myristate. This exposes the lipid group transiently and allows it to associate either with host membranes or a proteinaceous ligand during a critical step of entry. Introducing hydrophilic changes to the residues in the extreme N terminus (arrowhead) may constrain the movement of the hydrophobic acyl chain. Antibodies, such as 7D11 (orange), may neutralize entry by binding to loop 1 and sterically hinder the myristate release. Conserved disulfide-bonded cysteines (green) are also shown.

its expressed proteins are properly disulfide bonded. According to the structure of L1 in complex with 7D11 (71), a number of the residues of the 7D11 epitope are held in position by the Cys34-Cys57 disulfide bond. Therefore, it was not surprising that both of the nonmyristoylated mutants exhibited significant changes in two different conformation-dependent epitopes, including that of 7D11, and that these changes were less drastic for the myristoylated mutant S6A (Table 3).

How does the amino-appended myristate moiety affect the structural contortions of residues which are distal from the N terminus? The conventional model for protein folding posits that during the initial stage of the process, hydrophobic residues collapse to form a compact core (19). The available structural information for L1 at the atomic level suggests that its myristate moiety, which is cotranslationally appended to L1 (22), is critical for establishing the hydrophobic core during folding. An internal hydrophobic pocket exists within the two known nonmyristoylated structures of L1 (70, 71). The crystallographers noted that in the crystal structure, the cavity is filled with an electron density likely to be the polyethylene glycol derived from the crystallization solution (70). They postulated that in the natural myristoylated protein, the acyl group likely is embedded in the pocket.

Indeed, one of the most conserved hydrophobic residues lining the cavity, F108, is located at the deepest end of the cavity, where it is ideally situated for interaction with the terminal methyl group of the lipid (Fig. 7). We discovered that even a conservative replacement of F108 with alanine resulted in the loss of conformation-dependent epitopes, changes in redox state, and the diminution of its capacity to restore infectivity, in manners which are reminiscent of the nonmyristoylated mutants. However, unlike G2A and S6D, the myristoyl group of F108A is present in the protein molecule. One explanation is that the lipid group of F108A, though attached to the polypeptide chain, is not rested stably within its cavity due to its weakened hydrophobic interaction with the mutant alanine residue. Although a more comprehensive mutagenesis study is warranted, it also appears that some residues within the pocket are more critical than others for structural integrity and for virion infectivity. Taken together, the structural and biochemical evidence suggest that myristate serves as a structural unit in the core of the protein and that the unit is important for the proper conformation and disulfide bonding of L1 during its processing in VACV-infected cells. Solving the crystallographic structure of a myristoylated form of L1 in the future will address the validity of this model for the structural position of the myristate.

Bisht et al. recently demonstrated that the G2A mutant is in a reduced state and is not recognized by the disulfide bond-sensitive MAb 7D11 (7). These results are in broad agreement with our analyses of G2A, where we saw the ablated reactivity of 7D11 to the redox-reduced G2A. The authors also showed that G2A was dispersed throughout the cytoplasm, while wild-type L1 was localized primarily in viral factories. The authors therefore postulated that the lipid modification is required for the targeting of L1 to viral membranes in the factories, where the VACV-encoded thiol oxidoreductases are situated for disulfide bonding and for proper protein conformation (67–69, 84). A similar concept for the role of the myristate was also formerly proposed by Ravanello and Hruby (56).

However, three available lines of evidence do not support this proposed function for myristate. Most directly, our analyses of purified virions of two nonmyristoylated mutants illustrate that these mutant proteins do not have difficulty localizing and being incorporated into mature viruses. Second, if these nonmyristoylated mutants are indeed misdirected from viral membranes, one would expect them to have lost their association with other viral membrane proteins. During morphogenesis, the assembly of EFC proteins is dependent on the formation of viral membranes (65). Our finding that both G2A and S6D still remain associated with EFC constituents as a complex is more consistent with the notion that the lipid is not required for the membrane targeting of L1. Lastly, myristoylated proteins which utilize their fatty acid for membrane anchoring or targeting are typically cytosolic proteins which lack transmembrane domains (10, 57, 58, 73).

It is likely that the myristate group is required for purposes other than as a structural component during protein folding. Perhaps during the host entry of the mature virion, the myristate moves out of its cavity to fulfill a second role. It is becoming increasingly clear that a diversity of viruses, such as hepatitis B

virus (12, 28, 45), Junín virus (88), lymphocytic choriomeningitis virus (62), and equine arteritis virus (75), have evolved to capitalize on the unique properties of myristate for efficient cell entry or membrane fusion. The viral membrane fusion protein(s) of VACV has yet to be identified, although the A17-A27 complex (41) and the EFC constituent H2 (50) have been proposed as candidates. Curiously, L1 does not resemble any of the known viral fusion proteins in structure. Antibodies generated against a myristoylated form of the L1(2-34) peptide did not neutralize VACV entry (C. H. Foo, J. C. Whitbeck, M. Ponce-de-León, G. H. Cohen, and R. J. Eisenberg, unpublished data), although it should be stressed that it is challenging to confirm that these antibodies do in fact bind to the lipid moiety, since myristoylated peptides are relatively insoluble in water. Circumventing this technical issue for the acylated short peptides and the future use of myristoylated L1 polypeptides will aid in elucidating the exact role of the myristoyl moiety during entry.

The role of the conserved N-terminal residues of L1 (the so-called myristoyl switch model). The myristoyl switch model has been used to describe the operative mechanism of several cellular myristoylated proteins, such as the photoreceptor-specific protein recoverin (4, 80). The myristate group of recoverin can adopt two distinct conformations: exposed and available to promote membrane binding or sequestered inside a hydrophobic binding pocket within recoverin. The transition between these two states is regulated by calcium (3, 81). Calcium binding to the cytosolic form of recoverin triggers major conformational changes in the protein, causing its hidden myristate to flip outside the protein and converting it to the membrane-bound state.

Here, we propose a myristate switch model to describe the operation of L1 during entry (Fig. 7). This proposal is in accordance with what was articulated by the crystallographers who solved the structure of L1 (70). In this model, the lipid moiety of L1 would be buried within the protein prior to cell host entry. Upon encountering the appropriate cellular signals during the entry process (such as receptor binding and/or low pH), the acyl chain will be expelled to perform its second function. Possible functions include (i) the binding of L1 to an EFC protein that it was not directly interacting with previously during its resting phase, (ii) insertion into the viral membrane, or (iii) insertion into the host membrane to act as an anchor for the subsequent fusion of the viral and host lipid bilayers. Either of the last two scenarios would be consistent with the observation by Ravanello et al. that the acylated N-terminal fragment of L1 can retarget a fusion protein to cell membranes (54). One potential avenue for lipid extrusion is for loop 1 of L1 to act as a hinge (Fig. 7, asterisk) and swing the myristate-containing α1 helix away from the core of the protein. In this format, MAbs which bind to the top of the protein would prevent loop 1 from changing its conformation and consequently will have a neutralizing effect on entry. In fact, neutralizing epitopes of multiple MAbs have been mapped to this portion of L1 (Fig. 1A and 7) (2, 71).

We have demonstrated that substitutions of two of the N-terminal residues (A4 and A5) which are not part of the myristoylation motif either abolished or drastically diminished the complementation of infectivity. Interestingly, all other phenotypes for A4D and A5D, including N-myristoylation and structural conformations, do not appear to be significantly affected (Table 3). Is it possible that A4 and A5 serve as a docking motif for the binding partners of L1? Preliminary studies indicate that N-terminal peptides of L1 do not compete with soluble L1 for cell binding and do not suppress VACV entry, even at high concentrations (C. H. Foo et al., unpublished). In this report, we have also shown that polyclonal antibodies targeted against this region do not neutralize host entry. These results suggest that the N terminus of L1 is not the region responsible for the cell binding of L1 or for recombinant forms of it to inhibit entry. Furthermore, A4D and A5D do associate with subunits of the EFC. In sum, these two important alanine residues are not likely to constitute the binding site for any of the interaction partners of L1, either viral or host in nature. One plausible role for these conserved alanines is that they are significant for the conformational changes that L1 undergoes during entry. In the myristoyl switch model, it is critical during the conformational change that the lipid is flexible enough to swivel around the axis of the N-terminal peptide it is connected to. As such, the introduction of hydrophilic aspartic acid residues close to where the hydrophobic myristate is linked to L1 (Fig. 7, arrowhead) would be expected to restrict this swiveling movement, ultimately deterring virus entry. The generation of paired cysteine mutants with disulfide bonds to limit the movement of α1 helix will help assess the veracity of this postulated model.

The panel of L1-specific MAbs and the creation of substitution mutants, coupled with two X-ray crystallographic structures of L1, provide a rich nucleus of resources for the in-depth functional analysis of this protein. Further studies of L1 will shed some light on how these large DNA viruses with multiple entry proteins employ unique strategies to enter a diversity of eukaryotic cells.

ACKNOWLEDGMENTS

Funding for this project was provided by National Institutes of Health grants R21-AI-53404 and AI48487 and NIAID Mid-Atlantic Regional Center of Excellence grant U54 AI057168.

We are grateful to Bernard Moss for providing the recombinant virus vL1Ri. We thank Stuart N. Isaacs, Robert P. Ricciardi, and John Gallagher for their helpful advice and technical support.

REFERENCES

1. **Abramoff MD, Magalhaes PJ, Ram SJ.** 2004. Image processing with ImageJ. Biophotonics Int. **11**:36–42.
2. **Aldaz-Carroll L, et al.** 2005. Physical and immunological characterization of a recombinant secreted form of the membrane protein encoded by the vaccinia virus L1R gene. Virology **341**:59–71.
3. **Ames JB, et al.** 1997. Molecular mechanics of calcium-myristoyl switches. Nature **389**:198–202.
4. **Ames JB, Tanaka T, Stryer L, Ikura M.** 1996. Portrait of a myristoyl switch protein. Curr. Opin. Struct. Biol. **6**:432–438.
5. Reference deleted.
6. **Bengali Z, Townsley AC, Moss B.** 2009. Vaccinia virus strain differences in cell attachment and entry. Virology **389**:132–140.
7. **Bisht H, Brown E, Moss B.** 2010. Kinetics and intracellular location of intramolecular disulfide bond formation mediated by the cytoplasmic redox system encoded by vaccinia virus. Virology **398**:187–193.
8. **Bisht H, Weisberg AS, Moss B.** 2008. Vaccinia virus L1 protein is required for cell entry and membrane fusion. J. Virol. **82**:8687–8694.
9. **Blouch RE, Byrd CM, Hruby DE.** 2005. Importance of disulphide bonds for vaccinia virus L1R protein function. Virol. J. **2**:91.
10. **Boutin JA.** 1997. Myristoylation. Cell Signal. **9**:15–35.
11. **Brown E, Senkevich TG, Moss B.** 2006. Vaccinia virus F9 virion membrane protein is required for entry but not virus assembly, in contrast to the related L1 protein. J. Virol. **80**:9455–9464.
12. **Bruss V, Hagelstein J, Gerhardt E, Galle PR.** 1996. Myristylation of the large surface protein is required for hepatitis B virus in vitro infectivity. Virology **218**:396–399.
13. **Capul AA, et al.** 2007. Arenavirus Z-glycoprotein association requires Z myristoylation but not functional RING or late domains. J. Virol. **81**:9451–9460.

14. **Chang SJ, Chang YX, Izmailyan R, Tang YL, Chang W.** 2010. Vaccinia virus A25 and A26 proteins are fusion suppressors for mature virions and determine strain-specific virus entry pathways into HeLa, CHO-K1, and L cells. J. Virol. **84**:8422–8432.
15. **Chiu WL, Lin CL, Yang MH, Tzou DL, Chang W.** 2007. Vaccinia virus 4c (A26L) protein on intracellular mature virus binds to the extracellular cellular matrix laminin. J. Virol. **81**:2149–2157.
16. **Chung CS, Hsiao JC, Chang YS, Chang W.** 1998. A27L protein mediates vaccinia virus interaction with cell surface heparan sulfate. J. Virol. **72**: 1577–1585.
17. **Cole C, Barber JD, Barton GJ.** 2008. The Jpred 3 secondary structure prediction server. Nucleic Acids Res. **36**:W197–W201.
18. **Condit RC, Moussatche N, Traktman P.** 2006. In a nutshell: structure and assembly of the vaccinia virion. Adv. Virus Res. **66**:31–124.
19. **Dill KA, et al.** 1995. Principles of protein folding–a perspective from simple exact models. Protein Sci. **4**:561–602.
20. **Eisenberg RJ, et al.** 1987. Complement component C3b binds directly to purified glycoprotein C of herpes simplex virus types 1 and 2. Microb. Pathog. **3**:423–435.
21. **Evan GI, Lewis GK, Ramsay G, Bishop JM.** 1985. Isolation of monoclonal antibodies specific for human c-myc proto-oncogene product. Mol. Cell. Biol. **5**:3610–3616.
22. **Farazi TA, Waksman G, Gordon JI.** 2001. The biology and enzymology of protein N-myristoylation. J. Biol. Chem. **276**:39501–39504.
23. **Fogg C, et al.** 2004. Protective immunity to vaccinia virus induced by vaccination with multiple recombinant outer membrane proteins of intracellular and extracellular virions. J. Virol. **78**:10230–10237.
24. **Foo CH, et al.** 2009. Vaccinia virus L1 binds to cell surfaces and blocks virus entry independently of glycosaminoglycans. Virology **385**:368–382.
25. **Franke CA, Reynolds PL, Hruby DE.** 1989. Fatty acid acylation of vaccinia virus proteins. J. Virol. **63**:4285–4291.
26. **Franke CA, Wilson EM, Hruby DE.** 1990. Use of a cell-free system to identify the vaccinia virus L1R gene product as the major late myristylated virion protein M25. J. Virol. **64**:5988–5996.
27. **Gottlinger HG, Sodroski JG, Haseltine WA.** 1989. Role of capsid precursor processing and myristoylation in morphogenesis and infectivity of human immunodeficiency virus type 1. Proc. Natl. Acad. Sci. U. S. A. **86**:5781–5785.
28. **Gripon P, Le Seyec J, Rumin S, Guguen-Guillouzo C.** 1995. Myristylation of the hepatitis B virus large surface protein is essential for viral infectivity. Virology **213**:292–299.
29. Reference deleted.
30. **Henderson DA.** 1987. Principles and lessons from the smallpox eradication programme. Bull. World Health Organ. **65**:535–546.
31. **Heraud JM, et al.** 2006. Subunit recombinant vaccine protects against monkeypox. J. Immunol. **177**:2552–2564.
32. **Hooper JW, Custer DM, Schmaljohn CS, Schmaljohn AL.** 2000. DNA vaccination with vaccinia virus L1R and A33R genes protects mice against a lethal poxvirus challenge. Virology **266**:329–339.
33. **Hooper JW, et al.** 2004. Smallpox DNA vaccine protects nonhuman primates against lethal monkeypox. J. Virol. **78**:4433–4443.
34. **Hsiao JC, Chung CS, Chang W.** 1999. Vaccinia virus envelope D8L protein binds to cell surface chondroitin sulfate and mediates the adsorption of intracellular mature virions to cells. J. Virol. **73**:8750–8761.
35. **Ichihashi Y.** 1996. Extracellular enveloped vaccinia virus escapes neutralization. Virology **217**:478–485.
36. **Ichihashi Y, Oie M.** 1996. Neutralizing epitope on penetration protein of vaccinia virus. Virology **220**:491–494.
37. **Ichihashi Y, Takahashi T, Oie M.** 1994. Identification of a vaccinia virus penetration protein. Virology **202**:834–843.
38. **Izmailyan RA, Huang CY, Mohammad S, Isaacs SN, Chang W.** 2006. The envelope G3L protein is essential for entry of vaccinia virus into host cells. J. Virol. **80**:8402–8410.
39. **Kennedy RB, Ovsyannikova I, Poland GA.** 2009. Smallpox vaccines for biodefense. Vaccine **27**(Suppl. 4):D73–D79.
40. **Knipe DM, et al (ed).** 2007. Fields virology, 5th ed. Lippincott Williams & Wilkins, Philadelphia, PA.
41. **Kochan G, Escors D, Gonzalez JM, Casasnovas JM, Esteban M.** 2007. Membrane cell fusion activity of the vaccinia virus A17-A27 protein complex. Cell Microbiol. **10**:149–164.
42. **Koshizuka T, Kawaguchi Y, Nozawa N, Mori I, Nishiyama Y.** 2007. Herpes simplex virus protein UL11 but not UL51 is associated with lipid rafts. Virus Genes **35**:571–575.
43. **Kyte J, Doolittle RF.** 1982. A simple method for displaying the hydropathic character of a protein. J. Mol. Biol. **157**:105–132.
44. **Lin CL, Chung CS, Heine HG, Chang W.** 2000. Vaccinia virus envelope H3L protein binds to cell surface heparan sulfate and is important for intracellular mature virion morphogenesis and virus infection in vitro and in vivo. J. Virol. **74**:3353–3365.
45. **Macrae DR, Bruss V, Ganem D.** 1991. Myristylation of a duck hepatitis B virus envelope protein is essential for infectivity but not for virus assembly. Virology **181**:359–363.
46. **Matsubara M, Nakatsu T, Kato H, Taniguchi H.** 2004. Crystal structure of a myristoylated CAP-23/NAP-22 N-terminal domain complexed with Ca2+/calmodulin. EMBO J. **23**:712–718.
47. **Mercer J, et al.** 2010. Vaccinia virus strains use distinct forms of macropinocytosis for host-cell entry. Proc. Natl. Acad. Sci. U. S. A. **107**:9346–9351.
48. **Moss B.** 2001. *Poxviridae*: the viruses and their replication, p 2849–2883. *In* Knipe DM, et al (ed), Fields virology, 4th ed. Lippincott Williams & Wilkins, Philadelphia, PA.
49. **Nelson GE, Sisler JR, Chandran D, Moss B.** 2008. Vaccinia virus entry/fusion complex subunit A28 is a target of neutralizing and protective antibodies. Virology **380**:394–401.
50. **Nelson GE, Wagenaar TR, Moss B.** 2008. A conserved sequence within the H2 subunit of the vaccinia virus entry/fusion complex is important for interaction with the A28 subunit and infectivity. J. Virol. **82**:6244–6250.
51. **Nichols RJ, Stanitsa E, Unger B, Traktman P.** 2008. The vaccinia virus gene I2L encodes a membrane protein with an essential role in virion entry. J. Virol. **82**:10247–10261.
52. **Ojeda S, Domi A, Moss B.** 2006. Vaccinia virus G9 protein is an essential component of the poxvirus entry-fusion complex. J. Virol. **80**:9822–9830.
53. **Ojeda S, Senkevich TG, Moss B.** 2006. Entry of vaccinia virus and cell-cell fusion require a highly conserved cysteine-rich membrane protein encoded by the A16L gene. J. Virol. **80**:51–61.
54. **Ravanello MP, Franke CA, Hruby DE.** 1993. An NH2-terminal peptide from the vaccinia virus L1R protein directs the myristylation and virion envelope localization of a heterologous fusion protein. J. Biol. Chem. **268**: 7585–7593.
55. **Ravanello MP, Hruby DE.** 1994. Characterization of the vaccinia virus L1R myristylprotein as a component of the intracellular virion envelope. J. Gen. Virol. **75**:1479–1483.
56. **Ravanello MP, Hruby DE.** 1994. Conditional lethal expression of the vaccinia virus L1R myristylated protein reveals a role in virion assembly. J. Virol. **68**:6401–6410.
57. **Resh MD.** 1999. Fatty acylation of proteins: new insights into membrane targeting of myristoylated and palmitoylated proteins. Biochim. Biophys. Acta **1451**:1–16.
58. **Resh MD.** 2006. Trafficking and signaling by fatty-acylated and prenylated proteins. Nat. Chem. Biol. **2**:584–590.
59. **Rux AH, et al.** 1998. Functional region IV of glycoprotein D from herpes simplex virus modulates glycoprotein binding to the herpesvirus entry mediator. J. Virol. **72**:7091–7098.
60. **Sandgren KJ, et al.** 2010. A differential role for macropinocytosis in mediating entry of the two forms of vaccinia virus into dendritic cells. PLoS Pathog. **6**:e1000866.
61. **Satheshkumar PS, Moss B.** 2009. Characterization of a newly identified 35-amino-acid component of the vaccinia virus entry/fusion complex conserved in all chordopoxviruses. J. Virol. **83**:12822–12832.
62. **Schrempf S, Froeschke M, Giroglou T, von Laer D, Dobberstein B.** 2007. Signal peptide requirements for lymphocytic choriomeningitis virus glycoprotein C maturation and virus infectivity. J. Virol. **81**:12515–12524.
63. **Schultz AM, Rein A.** 1989. Unmyristylated Moloney murine leukemia virus Pr65gag is excluded from virus assembly and maturation events. J. Virol. **63**:2370–2373.
64. **Senkevich TG, Moss B.** 2005. Vaccinia virus H2 protein is an essential component of a complex involved in virus entry and cell-cell fusion. J. Virol. **79**:4744–4754.
65. **Senkevich TG, Ojeda S, Townsley A, Nelson GE, Moss B.** 2005. Poxvirus multiprotein entry-fusion complex. Proc. Natl. Acad. Sci. U. S. A. **102**: 18572–18577.
66. **Senkevich TG, Ward BM, Moss B.** 2004. Vaccinia virus entry into cells is dependent on a virion surface protein encoded by the A28L gene. J. Virol. **78**:2357–2366.
67. **Senkevich TG, Weisberg AS, Moss B.** 2000. Vaccinia virus E10R protein is associated with the membranes of intracellular mature virions and has a role in morphogenesis. Virology **278**:244–252.

68. **Senkevich TG, White CL, Koonin EV, Moss B.** 2002. Complete pathway for protein disulfide bond formation encoded by poxviruses. Proc. Natl. Acad. Sci. U. S. A. **99**:6667–6672.
69. **Senkevich TG, White CL, Koonin EV, Moss B.** 2000. A viral member of the ERV1/ALR protein family participates in a cytoplasmic pathway of disulfide bond formation. Proc. Natl. Acad. Sci. U. S. A. **97**:12068–12073.
70. **Su HP, et al.** 2005. The 1.51-Angstrom structure of the poxvirus L1 protein, a target of potent neutralizing antibodies. Proc. Natl. Acad. Sci. U. S. A. **102**:4240–4245.
71. **Su HP, Golden JW, Gittis AG, Hooper JW, Garboczi DN.** 2007. Structural basis for the binding of the neutralizing antibody, 7D11, to the poxvirus L1 protein. Virology **368**:331–341.
72. **Takasaki A, Hayashi N, Matsubara M, Yamauchi E, Taniguchi H.** 1999. Identification of the calmodulin-binding domain of neuron-specific protein kinase C substrate protein CAP-22/NAP-22. Direct involvement of protein myristoylation in calmodulin-target protein interaction. J. Biol. Chem. **274**:11848–11853.
73. **Taniguchi H.** 1999. Protein myristoylation in protein-lipid and protein-protein interactions. Biophys. Chem. **82**:129–137.
74. **Tessier DC, Thomas DY, Khouri HE, Laliberte F, Vernet T.** 1991. Enhanced secretion from insect cells of a foreign protein fused to the honeybee melittin signal peptide. Gene **98**:177–183.
75. **Thaa B, et al.** 2009. Myristoylation of the arterivirus E protein: the fatty acid modification is not essential for membrane association but contributes significantly to virus infectivity. J. Gen. Virol. **90**:2704–2712.
76. **Townsley AC, Senkevich TG, Moss B.** 2005. The product of the vaccinia virus L5R gene is a fourth membrane protein encoded by all poxviruses that is required for cell entry and cell-cell fusion. J. Virol. **79**:10988–10998.
77. **Townsley AC, Senkevich TG, Moss B.** 2005. Vaccinia virus A21 virion membrane protein is required for cell entry and fusion. J. Virol. **79**:9458–9469.
78. **Turner PC, et al.** 2007. Vaccinia virus temperature-sensitive mutants in the A28 gene produce non-infectious virions that bind to cells but are defective in entry. Virology **366**:62–72.
79. **Utsumi T, et al.** 2004. Vertical-scanning mutagenesis of amino acids in a model N-myristoylation motif reveals the major amino-terminal sequence requirements for protein N-myristoylation. Eur. J. Biochem. **271**:863–874.
80. **Valentine KG, Mesleh MF, Opella SJ, Ikura M, Ames JB.** 2003. Structure, topology, and dynamics of myristoylated recoverin bound to phospholipid bilayers. Biochemistry **42**:6333–6340.
81. **Weiergraber OH, Senin II, Philippov PP, Granzin J, Koch KW.** 2003. Impact of N-terminal myristoylation on the Ca2+-dependent conformational transition in recoverin. J. Biol. Chem. **278**:22972–22979.
82. **Welker R, Harris M, Cardel B, Krausslich HG.** 1998. Virion incorporation of human immunodeficiency virus type 1 Nef is mediated by a bipartite membrane-targeting signal: analysis of its role in enhancement of viral infectivity. J. Virol. **72**:8833–8840.
83. **Whitbeck JC, Foo CH, Ponce de Leon M, Eisenberg RJ, Cohen GH.** 2009. Vaccinia virus exhibits cell-type-dependent entry characteristics. Virology **385**:383–391.
84. **White CL, Weisberg AS, Moss B.** 2000. A glutaredoxin, encoded by the G4L gene of vaccinia virus, is essential for virion morphogenesis. J. Virol. **74**:9175–9183.
85. **Wolfe CL, Ojeda S, Moss B.** 2012. Transcriptional repression and RNA silencing act synergistically to demonstrate the function of the eleventh component of the vaccinia virus entry-fusion complex. J. Virol. **86**:293–301.
86. **Wolffe EJ, Vijaya S, Moss B.** 1995. A myristylated membrane protein encoded by the vaccinia virus L1R open reading frame is the target of potent neutralizing monoclonal antibodies. Virology **211**:53–63.
87. **Xiao Y, et al.** 2007. A protein-based smallpox vaccine protects mice from vaccinia and ectromelia virus challenges when given as a prime and single boost. Vaccine **25**:1214–1224.
88. **York J, Romanowski V, Lu M, Nunberg JH.** 2004. The signal peptide of the Junin arenavirus envelope glycoprotein is myristoylated and forms an essential subunit of the mature G1-G2 complex. J. Virol. **78**:10783–10792.